International Journal of GEOMATE, Nov., 2019 Vol.17, Issue 63, pp. 1 - 8
ISSN: 2186-2982 (P), 2186-2990 (O), Japan, DOI: https://doi.org/10.21660/2019.63.8227
Geotechnique, Construction Materials and Environment

DEVELOPMENT OF THE DEFORMATION MONITORING SYSTEM WITH WIRELESS SENSOR NETWORK AND EVALUATION OF MECHANICAL STABILITY FOR DAMAGED STONEWALLS

Yuuya Katsuda[1], Satoshi Sugimoto[1], Yoichi Ishizuka[1], Shohei Iwasaki[1], Ryoma Takaesu[1], Minoru Yamanaka[2]

[1]Faculty of Engineering, Nagasaki University, Japan;
[2]Faculty of Engineering, Kagawa University, Japan

*Corresponding Author, Received: 27 Jan. 2019, Revised: 18 Feb. 2019, Accepted: 26 March. 2019

ABSTRACT: Kumamoto Castle has constructed about 400 years ago, and now Cultural Affairs Agency of Japan treats as an important historical spot. The 2016 Kumamoto Earthquake was damaged a lot of stonewalls of this castle. Authors continue to investigate the deformation of unstable stonewalls by high accuracy laser module for measuring distance. And these stonewalls should be monitored continuously for the evaluation of mechanical stability, so we developed and established the wireless network system for measuring the changing angle of some stonewalls surface in this castle. The characteristics of this system are low cost and low power consumption with small-scale electric generation and a simple server. Authors also carried out making the simulation model and calculation for evaluation of stonewalls stability by the distinct element method under the several conditions of stonewall shape and interface of materials. The failure area of stonewalls and backfill are estimated by these results of the simulation, and it is discussed that these areas should be reinforced under repair of damaged stonewalls.

Keywords: Kumamoto Castle, Stonewalls, Wireless sensor network, Numerical simulation

1. INTRODUCTION

The 2016 Kumamoto earthquake gave huge damage to several structures in Japan. Kumamoto Castle was also damaged on architectural structures, stonewall, embankment and so on. The number of damaged stonewalls and embankment is over hundreds especially as shown in Fig. 1 [1], [2]. Therefore, the evaluation method of the stonewall and embankment stabilization is required from the view of geotechnical engineering quickly.

Kumamoto Castle has constructed about 400 years ago, and now the Cultural Affairs Agency of Japan treats as an important historical spot. Authors continue to investigate the deformation of unstable stonewalls by high accuracy laser module for measuring distance [1][3][4]. And these stonewalls should be monitored continuously for the evaluation of mechanical stability, so we developed and established the wireless network system for measuring the changing angle of some stonewalls surface in this castle. The characteristics of this system are low cost and low power consumption with small-scale electric generation and a simple server [5][6][7].

Authors also carried out making the simulation model and calculation for evaluation of stonewalls stability by the extended distinct element method under the several conditions of stonewall shape and interface of materials. The failure area of stonewalls and backfill are estimated by these results of the simulation, and it is discussed that these areas should be reinforced under repair of damaged stonewalls.

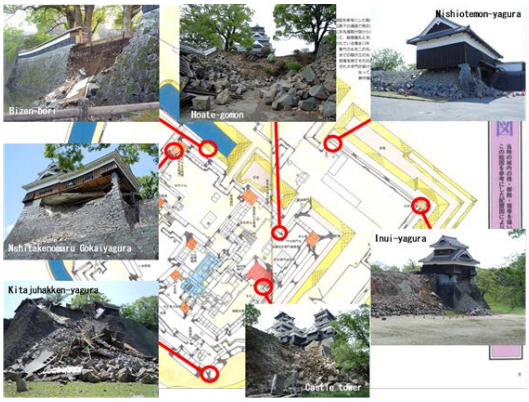

Fig.1 Several damages of Kumamoto Castle

2. OVERVIEW OF MONITORING SYSTEM

Our research team tried to mount the deformation monitoring system for evaluation of stonewall stability in Kumamoto Castle. The proposed system for monitoring is named MIST, which stands for Maintenance solution for Infrastructure and Slopes with Telecommunication [7]. The proposed remote monitoring system, shown in Fig. 2, is using ZigBee which is an IEEE 802.15.4-based specification for a suite of communication protocols. One of MIST is composed of (a) coordinator, (b) router and (c) end-device shown in Fig. 3. Each terminal has own

ZigBee chip. Recently, with the spread of the Internet of Things (IoT), various wireless communication standards are established. In the various standards, ZigBee has the feature like realizing over 60,000 connection and very low power consumption. Moreover, by using a sleep mode of Zigbee, it is possible to collect the necessary data and suppress power consumption. Further, by wireless communication using multi-hop, it is possible to use a plurality of communication paths, the overall system flexibility, stability is improved. Therefore, ZigBee is suitable for such a sensor network which requires multiple terminals and connections, also powered by standalone energy supply [3]. The voltage value obtained by the sensors at end-devices is converted to 16bit data by ADC in the end devices. The data is transmitted to the coordinator (master unit) via some routers (repeaters). This action is happened periodically, like once in 30 minutes. At the coordinator, which is tiny microcomputer (Raspberry Pi), all the data is transmitted to the remote host computer via the internet. The sensor devices are connected to end-devices with analog via ADC or digital via I2C. Each terminal is activated by own solar panel and Li-ion battery. Thus, the proposed MIST system can provide not only remote monitoring of long-distance location but also real-time analysis. Also, the analyzed data or sensed raw data can be accessed via the internet. The actual screenshot is shown in Fig.7.

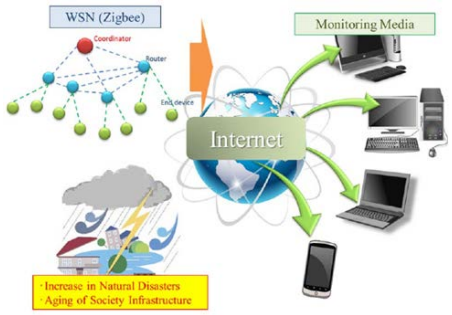

Fig.2 Image of Proposed System (MIST)

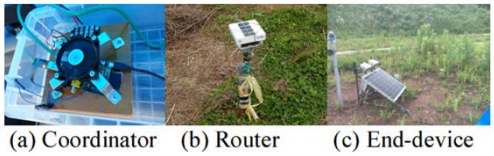

Fig.3 Terminal Devices

2.1 Application of MIST system for Kumamoto Castle

The 2016 Kumamoto earthquake gave huge damage for several earth structures in Kumamoto Castle. There are a lot of damage cases, for example, floating out of stonewalls, cracking of embankments as shown in Fig.4 & 5. These will be concerns in the future on instability as earth structures. In this study, the MIST system was constructed and operated on trial in the specific area of Kumamoto Castle for monitoring these damaged structures. Now some wireless sensors with gyroscope function were set on the top of damaged stonewalls, and it was confirmed that these apparatuses continued to work and collect displacement data stably.

Fig.4 Floating stonewall

Fig.5 Cracking embankment

Fig.6 shows the installation positions of end devices, routers, and coordinators installed in the unstable stonewall existing around Iida-maru and Takeno-maru in Kumamoto Castle. Here, routers for relaying communications are arranged as shown in this figure, in order to monitor the stonewalls at 5 places in total at two locations separated by a single distance of about 100 m from the coordinator. Since it was considered that the distance between equipment based on the result of field intensity measurement at the site, the height difference, the surrounding stonewalls and the existence of trees were each considered to affect the stability of communication. We also installed two routers at the

same spot to improve the relay stability of communication. The first equipment installation in November 2017, the second installation in January 2018, and as of the end of this fiscal year, the equipment arrangement shown in Fig.7 is adopted. In addition, an example of displaying the communication status on the web is shown in Fig.8.

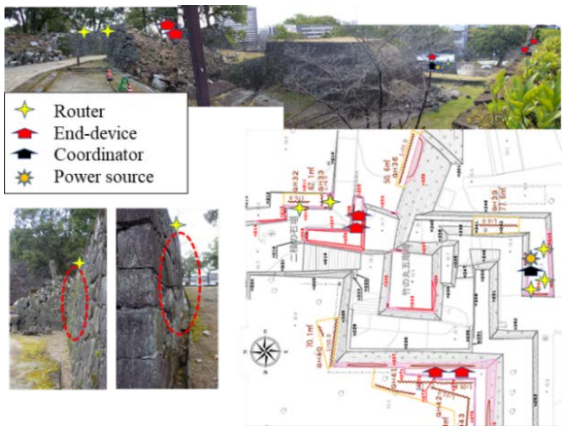

Fig.6 Location of each monitoring devices in the test field

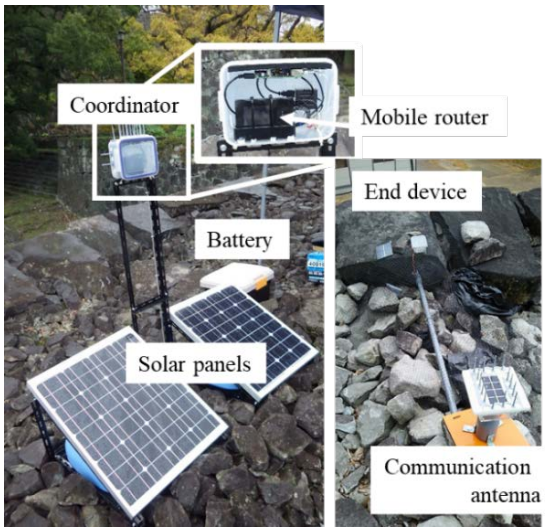

Fig.7 Monitoring devices

During the measurement of about 3 months, environmental conditions such as sunshine and outdoor temperature were bad conditions, and due to malfunction of power generation of the solar panel installed in each equipment and charging/discharging of the lithium-ion battery Communication stoppage which is thought to have occurred. Therefore, as shown in Fig.9, stable monitoring was not reached, but improvements will be made by increasing the solar panel and changing the battery type.

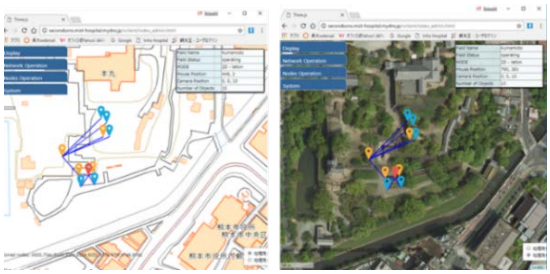

Fig.8 View of communication situation on the web browser

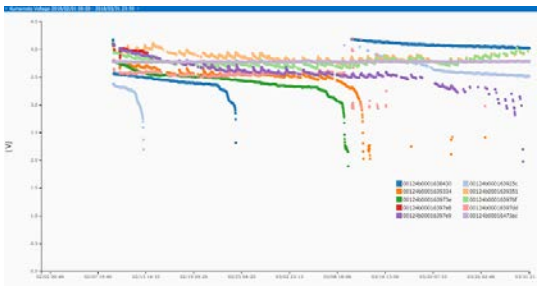

Fig.9 View of output voltage process for two months

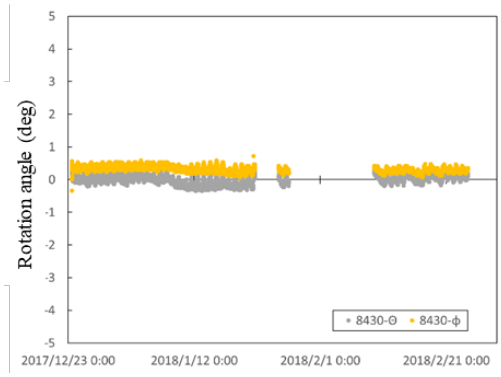

Fig.10 Results of the rotation angle of a gyro sensor

It is possible to calculate the rotation angle of stone based on the output change of the gyro sensor mounted on the communication module. As an example of the monitoring result, Fig.10 shows the change of the rotation angle of the module ID: 8430 where data was collected by relatively stable communication. The observation period is from 23 December 2017 to 24 February 2018, and the rotation angle in two directions is calculated from the beginning of the period. On the way, it can be confirmed that although there is data loss due to disruption of communication, it is almost unchanged in rotation angle. On the other hand, it is considered that the fact that the glass rod for confirming the occurrence of deformation occurred on the side of the stone wall from the current year does not occur at present has a stable condition as shown in Fig.11. In the future, we plan to continue

the validity of the output data of the module together with the result of regularly fixed point observation of the stone wall section by the laser rangefinder.

Fig.11 Glass rods for monitoring displacement between stones

(a) Situation before the disaster

(b) Situation after the disaster

Fig.12 Failure the stonewall of H323

3. THE STONE WALL MODELING AND CALCULATION BASED ON DYNAMIC NUMERICAL SIMULATION

3.1 Selection of target location for model

The model was selected from 60 stonewalls which were targeted at the survey of the damage situation of Kumamoto Castle. The selection terms are as follows. The first is that the height of the stonewall is 10 meters or more. The second is that collapse is occurring in the central part of the stonewall. Third, there is information on the shape in past literature. Based on the above conditions, we selected part number H323 as the object of the model. Fig.12 shows the model H323 before and after the disaster. The figure shows that H323 collapsed only at the central part of the stonewall. In H323 there was data of the shape before the earthquake in F.Kuwahara " The gradient of the stone walls in Kumamoto Castle "[8]. We created the shape of the model with reference to this literature.

3.2 Overview of the model

Fig.13 shows the setting element condition of the model. The area of the embankment was set as an elasto-plastic element. The area of the stone and the bedrock were set as rigid elements. Between the stonewall and the embankment were set as joint elements.

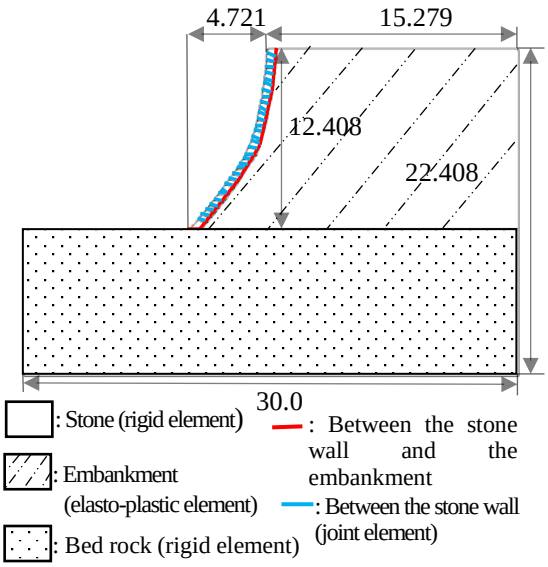

Fig.13 Element condition of the model (unit: meter)

3.3 The boundary condition of the model

The important point is setting boundary conditions on dynamic numerical simulations. In order to reproduce the seismic motion, we set the boundary condition shown in Fig.14 A dashpot was provided at the bottom of the model. The boundary surface becomes a viscous boundary by a dashpot.

Below the boundary, surface is expressed as semi-infinite ground by a viscous boundary. The semi-infinite ground absorbs the escaping wave energy. It is possible to input only the rising wave component of the seismic wave by absorbing the wave energy. We set free rock area on the side of the model. We set an energy transfer boundary between the free rock area and
model. The energy transfer boundary transmits the escaping wave energy to the free rock area. The free rock area absorbs the escaping wave energy. By this effect, the side of the boundary surface is expressed as a semi-infinite ground [9].

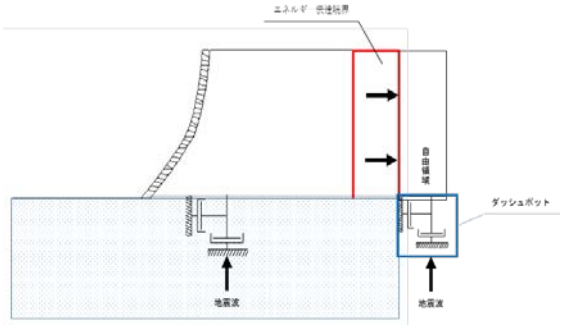

Fig.14 Overview of boundary condition

3.4 Setting up of model's characteristic value

Table 1 shows the physical properties of stone and embankment in the model. Table 2 shows the physical property value of the joint element. Since the target model collapsed at the upper part of the stone wall, it is considered that the stress in the vertical direction was small from the viewpoint of Mohr-Coulomb's failure criterion. Therefore, it is considered that the influence of the angle of shear resistance is small. On the other hand, it is considered that the influence of the cohesion of embankment is large. For the above reason, we divided the cohesion of embankment into 3 cases. (Table 3)

Table 1 Physical property value of block element

Item	Embankment	Stone
Density(g/cm^3)	2.5	2.75
Elastic Coefficient E(MPa)	55	5.5×10^4
Poisson's ratio ν	0.1	0.2
Cohesion c(KPa)	Refer to Table 3	7.0×10^2
Internal Frictional Angle φ(°)	40	45
Tensile Strength σ(MPa)	350	7.0×10^6

Table 2 Phusical property value of joint element

Item	Between embankment and stone	Between each stone
Cohesion c(KPa)	35	350
Internal friction angle φ(°)	35	40
Tensile strength σ_t(MPa)	350	35

Table 3 Cohesion of embankment

Cohesion (KPa)	Case 1	Case 2	Case 3
	0.0	15.0	50.0

3.5 On the seismic velocity waveform applied to the model

When doing dynamic numerical simulation, it is necessary to input the observed earthquake record. We used the main shock of the Kumamoto earthquake that occurred on April 16. The seismic wave characteristics of the main shock were obtained from "Kyoshin Net" (K-net) of National Research Institute for Earth Science and Disaster Resilience [10]. "KMM006 Kumamoto" was selected as an observed earthquake record. Fig.15 shows the observation point of "KMM006 Kumamoto".

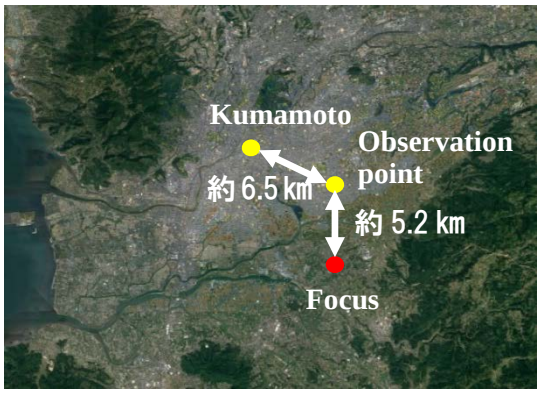

Fig.15 Observation station

Fig.16 shows the velocity waveform of the observed earthquake record. The maximum speed of the velocity waveform NS component is 61.6 cm/sec. The maximum speed of the velocity waveform EW component is 79.9 cm/sec. The maximum speed of the velocity waveform UD component is 27.0 cm/sec. The NS component means the waveform in the north-south direction of the seismic waveform. Similarly, the EW component means the waveform in the east-west direction, and the UD component means the waveform in the vertical direction.

In the model H323, the direction of the

stonewall is the south direction. For that reason, the NS component was used as the velocity component in the shear direction. 0.0 to 15.0 seconds at which the maximum waveform is observed was used as the input waveform

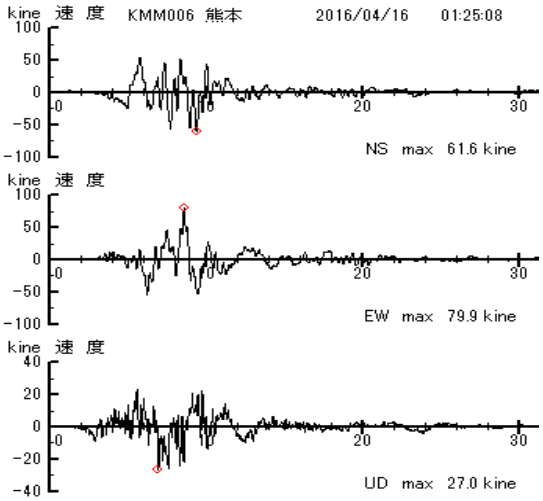

Fig.16 Seismic velocity waveform in Kumamoto

4. RESULT OF SIMULATION AND DISCUSSION

4.1 Displacement Vector

Fig.17, 18, 19 show the simulation results of the displacement vector. The displacement to the outside of the stonewall was confirmed in all cases. In case 1 (cohesion 0 KPa), the embankment of the upper part of stonewall collapses to the stone wall side. The maximum displacement is 5.1 meters. In case 2 (cohesion 15 KPa), the embankment of the upper part of the stonewall is the largest displaced. But case 2 did not collapse. The maximum displacement is 0.12 meters. In the case3 (cohesion50KPa), large displacement was not confirmed. However, case 3 was a larger displacement than case 2. The maximum displacement is 0.15 meters.

In Case 1, it is considered that the embankment caused plastic deformation at the time of gravity analysis. On the other hand, in case 2 and 3, the top of the embankment confirmed an upward displacement of 0 to 13 centimeters. It is considered that the top of the embankment has not set as a viscous boundary.

4.2 Elastic fracture

Fig.20, 21, 22 show the simulation results of elastic fracture. The phenomenon shown in this figure expresses the collapse situation of the embankment, which is the elasto-plastic model. Red

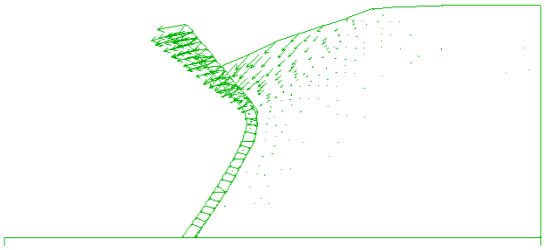

Maximum displacement of 5.1 m

Fig.17 Displacement vector of cohesion 0 KPa

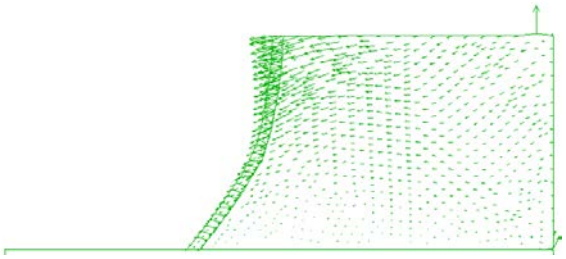

Maximum displacement 0.12m

Fig.18 Displacement vector of cohesion 15 KPa

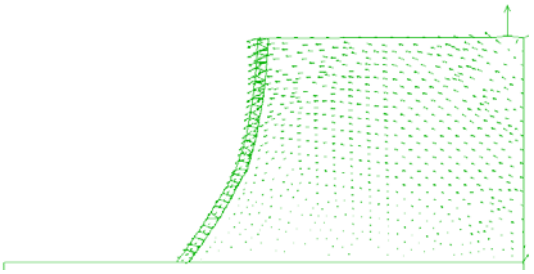

Maximum displacement 0.15m

Fig.19 Displacement vector of cohesion 50 KPa

is plastic failure, purple is tensile failure, green is expressed as past failure points.

In case 1 (cohesion 0KPa), the whole embankment was destroyed after about 1 second with the starting shaking. The plastic failure occurred in the embankment of the upper part of stonewall. After that, the embankment on the upper part of stonewall collapsed with tensile failure.

In case 2 (cohesion 15KPa), the embankment surface has already destroyed in 1 second. It is considered that this cause is gravity analysis before the main simulation. Because the surface of the embankment received the load of the stone. After that, plastic failure gradually occurred from the embankment in the lower part of stonewall. The tensile failure occurred in the embankment of the top of stonewall in the end.

In case 3 (cohesion 50KPa), it is found that the failure range is narrower than case 2. Plastic failure of the lower part of stonewall was later than Case 2. From this result, it is understood that the influence

on the embankment is relatively small.

As a collapse mechanism inside the embankment, it was found that collapse progresses on the embankment surface due to plastic fracture. When exceeding a certain range of failure on the surface of the embankment, tensile failure occurs in the embankment of the upper part of the stonewall. As a result, active earth pressure occurred in the upper part of stonewall.

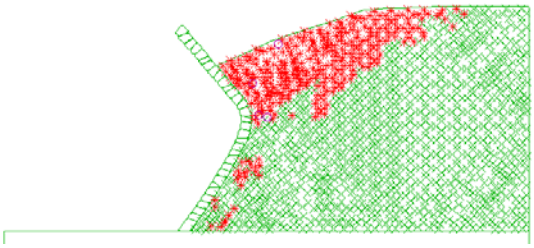

Fig.20 Plastic failure of cohesion 0 KPa

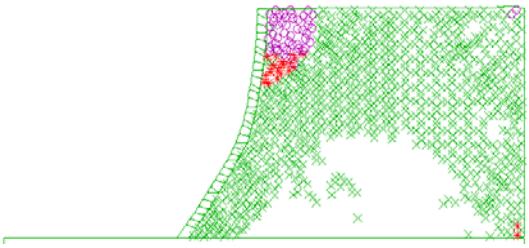

Fig.21 Plastic failure of cohesion 15 KPa

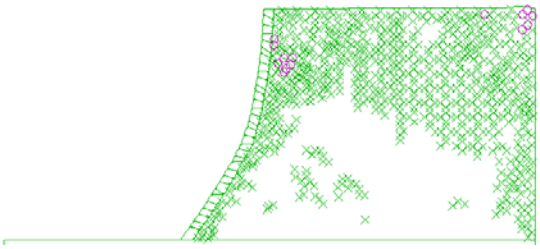

Fig.22 Plastic failure of cohesion 50 KPa

5. CONCLUSION

In this paper, we described the construction and operation of a monitoring system aimed at evaluating the stability of the stonewall damaged by a huge earthquake and numerical calculation by the distinct element method. This monitoring system is realized by diverting and extending what the authors developed for evaluating the stability of the slope. The current situation has problems in securing communication stability and securing power supply. However, since measurement with a gyro sensor is realized, it is necessary to improve these problems.

In the analysis, the stonewall collapse was caused by the change in the cohesion of the embankment, so it was found that the cohesion was one of the factors for the stone wall collapse mechanism. The factor for the collapse that the plastic fracture of the embankment close to the stonewall surface and the tensile fracture on the ground surface of the embankment. When the maximum velocity waves for earthquake had passed, plastic and tensile failure simultaneously occurred in the embankment of the stonewall, and active earth pressure was generated. Due to this collapse mechanism, the failure of embankment gradually extends from the ground surface. When destruction progresses had passed, a large displacement occurs as in adhesive. We presumed that the stonewall has collapsed due to the displacement of the embankment.

6. ACKNOWLEDGMENTS

The authors gratefully appreciate a lot of support and understanding for this investigation from all officers of Kumamoto Castle Survey and Research Center after shortly after the 2016 Kumamoto earthquake. Our gratitude extends to all cooperators of this investigation with several instruments and information.

And this research is carried on by The Taisei Foundation on financial support.

7. REFERENCES

[1] Sugimoto S., M. Yamanaka, H. Maeda, N. Fukuda, Y. Katsuda: Research of damaged condition by the 2016 Kumamoto Earthquake and ground investigation on stone walls and earth structures in Kumamoto Castle, International Journal of GEOMATE, Vol.14, Issue 45, pp.66-72, 2018.

[2] Sugimoto S., M. Yamanaka.: Reports of damaged earth structures in Kumamoto Castle, Proceedings of 54th Natural disaster and science symposium, pp.45-51 (in Japanese), 2017.

[3] Katsuda Y., Y.Jiang, K. Omine, S.Sugimoto: Research of damaged stone structures in Kumamoto Castle by the 2016 Kumamoto Earthquake, Proceedings of 72th JSCE conference (CD-ROM), pp.479-480 (in Japanese), 2017.

[4] Katsuda Y., S. Sugimoto, M. Yamanaka: Reports of a survey on damaged stonewalls in Kumamoto Castle by the 2016 Kumamoto Earthquake, Proceedings of the Japan National

Conference on Geotechnical Engineering, in submission (in Japanese), 2018.

[5] Sugimoto S., T. Sasamura, J. Ishida, Y. Ishizuka, T. Fujishima, T. Fujimoto, S. Iwasaki, K. Yamashita, K. Kurihara: Development and application of slope monitoring system by a wireless sensor network, Proceedings of 71st JSCE conference (CD-ROM), pp.27-28 (in Japanese), 2016.

[6] Chang H., J. Ishida, S. Sugimoto, Y.Jiang, K. Omine, Y. Ishizuka, T. Sasamura, S. Iwasaki: Application of slope monitoring system by a wireless sensor network, Proceedings of 72th JSCE conference (CD-ROM), pp.67-68. (in Japanese), 2017.

[7] Nishikawa Y., T. Sasamura, Y. Ishizuka, S. Sugimoto, S. Iwasaki, H. Wang, T. Fujishima, T. Fujimoto, K. Yamashita, T. Suzuki, K. Kurihara: Design of Stable Wireless Sensor Network for Slope Monitoring, Proceedings of 2018 IEEE Topical Conference on Wireless Sensors and Sensor Networks(CDROM), TU3P-18, pp.8-11, 2018.

[8] Kuwahara F.: The gradient of the stone walls in Kumamoto Castle, Report of researches / Nippon Institute of Technology, 14-2, pp.59-74. (in Japanese), 1984.

[9] Fujii I., L. Yang, Y. Jiang, S. Li, T. Tanahashi: Evaluation of the dynamic behaviors of the bedrock containing discontinuities under important buildings based on numerical simulations, Proceedings of 2011 JSCE west conference (CD-ROM), pp.411-422(in Japanese), 2011.

[10] National Research Institute for Earth and Disaster Resilience “K-NET”, http:www.kyoshin.bosai.go.jp/kyoshin/, 2017.